Robust Observer Backstepping Neural Network Control of Flexible-Joint Manipulator

Withit Chatlatanagulchai, Hyuk Chul Nho, and Peter H. Meckl

Abstract—**An output-feedback controller design for flexible-joint manipulators is presented. The proposed controller design consists of a nonlinear Luenberger-type observer, multilayer neural network plant identifier, and controller based on a backstepping framework and variable structure controller. Only link angular positions are measured as outputs. The controller achieves good performance despite the presence of additive external disturbances, unmodeled dynamics, actuator nonlinearities, i.e., deadzone and backlash, and payload changes. Simulation of a two-link flexible-joint manipulator is included.**

I. Introduction

DYNAMIC modeling and control design of flexible-joint manipulators have attracted the attention of many researchers due to the fact that joint flexibility is one of the major obstacles in the design of high performance motion controls for industrial robots [1]. Sources of joint flexibility arise from driving components such as actuators, gear teeth, transmission belts, or transducers inserted in joints to measure joint torque. Thus, if high performance is required, joint flexibility should be taken into account in both modeling and control design.

Controller design for flexible-joint manipulators is quite a challenging problem. Besides being a highly coupled nonlinear system, the system is under-actuated, i.e., the number of control inputs is less than the degrees of freedom, which prohibits each link to be directly actuated by the torque input. In addition, the system possesses hard nonlinearities in the form of friction, deadzone and backlash [2]. In operation, the manipulator is usually also subjected to external disturbances, both repetitive and non-repetitive. In some situations, it is also impossible technically or economically to have sensors for all states. Moreover, the system is usually time varying due to payload changes.

In the past, several control design schemes have been proposed for control of flexible-joint manipulators based on such design frameworks as backstepping, passivity-based, singular perturbation and intelligent techniques such as fuzzy logic and neural networks. Comparison among various backstepping and passivity-based controllers based on cascaded plant is presented in [3]. Control design based on singular perturbation can be found in [4], [5], [6]. Intelligent techniques used for plant identifiers are reported in [7], [8]. All previous works are based on some rather restricted assumptions, such as unknown plant parameters must be linearly parametrizable, acceleration or force must be measured, plant is known exactly, disturbances are allowed only at input channels, system must be autonomous, etc.

The controller design technique used in this paper is presented by the authors in [9]. Fig. 1 depicts the system block diagram. Multilayer neural networks are used to identify unknown plant functions using their universal approximation properties. Nonlinear Luenberger-type observer is used to estimate unmeasured states. This enables us to design a controller using only link angular position measurement. Controller structure is based on backstepping technique. Robustness is provided by variable structure controller. The plant being controlled is a two-link flexible joint manipulator subjected to external additive disturbances. Extension to more links can be done naturally and is not presented here. We include actuator nonlinearities, i.e., deadzone and backlash, and a reasonable friction model, as proposed in [13], in the plant used in our simulation. The control objective is to track a desired trajectory while payload changes.

The paper is organized as follows. Section II contains the system description. Section III contains identifier, observer and controller designs. Section IV presents simulation results and Section V is the conclusion.

II. System Description

Fig. 2 depicts the schematic of a two-link planar flexible joint manipulator. Links are driven by motors via chains and sprockets. Each joint has a linear torsional spring to provide flexibility. The second motor and sprocket are attached to the first link.

A. Dynamics Model

Lagrange's method is used in deriving the mathematical model. Details of the derivation can be found in [10].

Manuscript received March 12, 2004.

The authors are with Motion and Vibration Control Laboratory, School of Mechanical Engineering, Purdue University, West Lafayette, IN 47907-2088 USA (e-mail: chatlata@purdue.edu, hnho@purdue.edu, meckl@purdue.edu; phone: 765-494-5686 ; fax: 765-494-0539).

Assumption 1: kinetic energy of the second motor and sprocket are mainly due to their pure rotation and neglect the rotation of the link.

Imposing Assumption 1 and letting $q_1 = [\theta_1 \;\; \theta_2]^T$ and $q_2 = [\theta_5 \;\; \theta_6]^T$, we then have the plant model in a more well-known form [11]:

$$\begin{aligned} &M(q_1)\ddot{q}_1 + V(q_1,\dot{q}_1)\dot{q}_1 + K(q_1 - q_2) = 0, \\ &J\ddot{q}_2 + B\dot{q}_2 - K(q_1 - q_2) = T, \end{aligned} \tag{2.1}$$

where $M(q_1)$ is inertia matrix, $V(q_1,\dot{q}_1)$ is Coriolis matrix, K is joint flexibility matrix, J represents the inertia of motors and sprockets, B represents internal damping of the torsional spring, and $T = [T_1 \;\; T_2]^T$ is the input torque vector.

B. Friction Model

A reasonable friction model [13] is as follows:

$$\begin{aligned} &\frac{d\xi}{dt} = \dot{\theta} - \frac{|\dot{\theta}|}{g(\dot{\theta})}\xi, \\ &\sigma_0 g(\dot{\theta}) = F_c + (F_s - F_c)e^{-(\dot{\theta}/v_s)^2}, \\ &F(\dot{\theta}) = \sigma_0\xi + \sigma_1\frac{d\xi}{dt} + \sigma_2\dot{\theta}, \end{aligned} \tag{2.2}$$

where $\sigma_0, \sigma_1, \sigma_2, F_c, F_s, v_s$ are unknown parameters usually obtained from experiment, ξ is the average deflection of the bristles in the micro scale, $\dot{\theta}$ is the relative angular velocity between the two surfaces, and F is the friction force that comprises coulomb friction, Stribeck effect, and viscous friction.

C. Deadzone Model

Deadzone is a static nonlinearity that describes insensitivity of the system to small input signals. Deadzone at the input to an actuator system, e.g., DC motor, is usually caused by friction and mechanical wear. Because a deadzone changes the characteristic of the desired control input, compensation is needed to remove its effect. Compensation schemes using multilayer neural networks can be found in [2]. The mathematical model of deadzone as in [12] is given as follows:

$$\tau = D(u) = \begin{cases} h_1(u) < 0, & u \le d_-, \\ 0, & d_- < u < d_+, \\ h_2(u) > 0, & u \ge d_+. \end{cases} \tag{2.3}$$

d_-, d_+ are unknown numbers and may be time-varying. $h_1(u)$ and $h_2(u)$ are unknown functions.

D. Backlash Model

The space between teeth on a mechanical gearing system must be made larger than the gear teeth width as measured on the pitch circle in order to avoid jamming when two gears are meshing. Backlash is the difference between tooth space and tooth width. Backlash results in a delay in the system motion. When the driving gear changes its position, the driven gear follows only after some delay. A backlash model as in [2] is given by

$$\dot{T} = B(T,\tau,\dot{\tau}) = \begin{cases} m\dot{\tau} & \text{if } \dot{\tau} > 0 \text{ and } T = m(\tau - d^+), \\ & \text{if } \dot{\tau} < 0 \text{ and } T = m(\tau - d^-), \\ 0 & \text{otherwise.} \end{cases} \tag{2.4}$$

d_-, d_+, m are unknown numbers.

E. Overall Plant Model

Fig. 3 depicts the overall plant model, where u is our designed control input, τ is output of the deadzone model, and T is output of the backlash model, which is input torque to actually drive the manipulator. Both τ and T are not measurable. Adding a friction model (2.2) to the dynamics model (2.1), we have the overall model as follows:

$$\begin{aligned} &M(q_1)\ddot{q}_1 + V(q_1,\dot{q}_1)\dot{q}_1 + K(q_1 - q_2) + F_1(\dot{q}_1) = 0, \\ &J\ddot{q}_2 + B\dot{q}_2 - K(q_1 - q_2) + F_2(\dot{q}_2) = T, \end{aligned}$$

where $F_1(\dot{q}_1) = [F(\dot{\theta}_1) \;\; F(\dot{\theta}_2)]^T$ and $F_2(\dot{q}_2) = [F(\dot{\theta}_5) \;\; F(\dot{\theta}_6)]^T$. Letting $x_1 = q_1, x_2 = \dot{q}_1, x_3 = q_2, x_4 = \dot{q}_2$, we can transform the model to strict feedback form as follows:

$$\begin{aligned} \dot{x}_1 &= x_2 + d_{a1}, \\ \dot{x}_2 &= f_2(x_1,x_2) + g_2(x_1,x_2)(x_3 + d_{a2}), \\ \dot{x}_3 &= x_4 + d_{a3}, \\ \dot{x}_4 &= f_4(x_1,x_2,x_3,x_4) + g_4(x_1,x_2,x_3,x_4)(T + d_{a4}), \\ y &= x_1, \end{aligned} \tag{2.5}$$

where $x_i, T \in \mathbb{R}^2$ and f_i, g_i are as follows:

$$\begin{aligned} &f_2 = -M(x_1)^{-1}\left[V(x_1,x_2)x_2 + F_1(x_2) + Kx_1\right], \\ &g_2 = M(x_1)^{-1}K, \\ &f_4 = -J^{-1}\left[Bx_4 - K(x_1 - x_3) + F_2(x_4)\right],\; g_4 = J^{-1}. \end{aligned}$$

Assumption 2: $d_{ai} \in C^1 \bigcap L^2_{\infty e}, \forall i = 1,\ldots,4,$ are additive uncertainties that may depend on some states and time and are bounded by

$$\left\|d_{aik}(\bar{x}_i,t)\right\| < d_{aikU}, \;\; \forall i = 1,\ldots,4, \;\; \forall k = 1,2,$$

where d_{aikU} are unknown.

III. Control System Design

Definition 1: $(\bullet^*) = (\hat{\bullet}) - (\tilde{\bullet})$, where $(\bullet^*)$ is actual value to be estimated, $(\tilde{\bullet})$ is estimated error and $(\hat{\bullet})$ is estimated value.

A. Identifier Design

Each unknown function in (2.5) is identified by one 3-layer NN as in Fig. 4 using its universal approximation property proved in [14]. Each variable in the network can be defined as follows:

$$\bar{Z} = [z_1, z_2, \ldots, z_n, 1]^T \in \mathbb{R}^{n+1},$$
$$V = [v_1, v_2, \ldots, v_l] \in \mathbb{R}^{(n+1)\times l},$$
$$v_i = [v_{i1}, v_{i2}, \ldots, v_{i(n+1)}]^T \in \mathbb{R}^{n+1}, i = 1, 2, \ldots, l,$$
$$g(W, V, Z) = W^T S(V^T \bar{Z}) \in \mathbb{R},$$
$$S(V^T \bar{Z}) = [s(v_1^T \bar{Z}), s(v_2^T \bar{Z}), \ldots, s(v_l^T \bar{Z}), 1]^T \in \mathbb{R}^{l+1},$$
$$W = [w_1, w_2, \ldots, w_l, w_{l+1}]^T \in \mathbb{R}^{l+1}.$$

$s(\bullet)$ can be any appropriate activation function. In this paper we use a sigmoid function $s(z_i) = 1/(1+e^{-z_i}), \forall z_i \in \mathbb{R}$.

Assumption 3: Any smooth nonlinear function, $g(z_1, z_2, \ldots, z_n) \in \mathbb{R}$, can be represented by a 3-layer NN with some constant ideal weight matrices, W^*, V^*, as follows:

$$g(z_1, z_2, \ldots, z_n) = W^{*T} S(V^{*T} \bar{Z}) + \varepsilon,$$

where $\|\varepsilon\| < \varepsilon_U$ is approximation error with unknown $\varepsilon_U > 0$.

Assumption 4: $\|W^*\| \le W_U$, $\|V^*\|_F \le V_U$, where W_U and V_U are not known.

The approximation of $g(z_1, z_2, \ldots, z_n)$ is given by

$$\hat{g} = \hat{W}^T S(\hat{V}^T \bar{Z}). \tag{3.1}$$

Lemma 1: The NN approximation error can be put in a linearly parameterized form in terms of $\tilde{W}$ and $\tilde{V}$ as

$$\hat{W}^T S(\hat{V}^T \bar{Z}) - W^{*T} S(V^{*T} \bar{Z}) = \tilde{W}^T (\hat{S} - \hat{S}' \hat{V}^T \bar{Z}) + \hat{W}^T \hat{S}' \tilde{V}^T \bar{Z} + d_u,$$
where $\hat{S} = S(\hat{V}^T \bar{Z}) \in \mathbb{R}^{l+1}$,
$$\hat{S}' = diag\{\hat{s}_1', \hat{s}_2', \ldots, \hat{s}_l', 0\} \in \mathbb{R}^{(l+1)\times(l+1)},$$
$$\hat{s}_i' = s'(\hat{v}_i^T \bar{Z}) = \left.\frac{d[s(z_a)]}{dz_a}\right|_{z_a = \hat{v}_i^T \bar{z}} \in \mathbb{R}, i = 1, 2, \ldots, l,$$
$s(z_i) = 1/(1+e^{-z_i}), \forall z_i \in \mathbb{R}$.

The residual term d_u is bounded by

$$|d_u| \le \|V^*\|_F \left\|\bar{z}\hat{W}^T \hat{S}'\right\|_F + \|W^*\| \left\|\hat{S}' \hat{V}^T \bar{z}\right\| + |W^*|_1.$$

Proof: See [15].

Replacing unknown functions in (2.5) with neural network estimates, we have

$$\begin{aligned}
\dot{x}_1 &= x_2 + d_{a1}, \\
\dot{x}_2 &= \hat{f}_2(\bar{x}_2) + \hat{g}_2(\bar{x}_2)(x_3 + d_{a2}), \\
\dot{x}_3 &= x_4 + d_{a3}, \\
\dot{x}_4 &= \hat{f}_4(\bar{x}_4) + \hat{g}_4(\bar{x}_4)(T + d_{a4}), \\
y &= x_1,
\end{aligned} \tag{3.2}$$

where

$$x_i \in \mathbb{R}^2 = [x_{i1}, x_{i2}]^T,\ T \in \mathbb{R}^2 = [T_1, T_2]^T,\ y \in \mathbb{R}^2 = [y_1, y_2]^T,$$
$$\bar{x}_i = \{x_1, x_2, \ldots, x_i\},$$
$$\hat{f}_i(\bullet) \in \mathbb{R}^2 = [\hat{f}_{i1}, \hat{f}_{i2}]^T,\ \hat{g}_i(\bullet) \in \mathbb{R}^{2\times 2} = \begin{bmatrix} \hat{g}_{i11} & \hat{g}_{i12} \\ \hat{g}_{i21} & \hat{g}_{i22} \end{bmatrix},$$
$$\hat{f}_{ij} = \hat{W}_{fij}^T S_{fij}(\hat{V}_{fij}^T \bar{Z}_{fij}) \in \mathbb{R},\ \hat{g}_{ijk} = \hat{W}_{gijk}^T S_{gijk}(\hat{V}_{gijk}^T \bar{Z}_{gijk}) \in \mathbb{R}.$$

B. Observer Design

To design an observer for plant (2.5), we proceed from mapping the states of the plant to the derivatives of the output y as follows:

$$y_e = \begin{bmatrix} y_{e11} \\ \vdots \\ y_{e14} \\ y_{e21} \\ \vdots \\ y_{e24} \end{bmatrix} = \begin{bmatrix} y_1 \\ \vdots \\ \ddot{y}_1 \\ y_2 \\ \vdots \\ \ddot{y}_2 \end{bmatrix} = H(\bar{x}_4) = \begin{bmatrix} x_{11} \\ \vdots \\ \varphi_{13}(\bar{x}_4) \\ x_{12} \\ \vdots \\ \varphi_{23}(\bar{x}_4) \end{bmatrix} = \begin{bmatrix} H_1(\bar{x}_4) \\ H_2(\bar{x}_4) \end{bmatrix}. \tag{3.3}$$

Assumption 5: The plant (2.5) is uniformly completely observable.

Proposition 1: Using a nonlinear observer [9] as follows:

$$\begin{bmatrix} \dot{\hat{x}}_1 \\ \dot{\hat{x}}_2 \\ \dot{\hat{x}}_3 \\ \dot{\hat{x}}_4 \end{bmatrix} = \begin{bmatrix} \hat{x}_2 \\ \hat{f}_2(\hat{\bar{x}}_2) + \hat{g}_2(\hat{\bar{x}}_2)\hat{\bar{x}}_3 \\ \hat{x}_4 \\ \hat{f}_4(\hat{\bar{x}}_4) + \hat{g}_4(\hat{\bar{x}}_4)T \end{bmatrix} + \left[\frac{\partial H(\hat{\bar{x}}_4)}{\partial \hat{\bar{x}}_4}\right]^{-1} \varepsilon^{-1} L[y - \hat{y}], \tag{3.4}$$
$$\hat{y} = \hat{x}_1,$$

where $\hat{\bar{x}}_i = \{\hat{x}_1, \hat{x}_2, \ldots, \hat{x}_i\}$, $\varepsilon_i = diag[\eta, \eta^2, \ldots, \eta^4]$, $0 < \eta \le 1$, $\varepsilon = block - diag[\varepsilon_1, \varepsilon_2] \in \mathbb{R}^{8\times 8}$.
$L = block - diag[L_1, L_2] \in \mathbb{R}^{8\times 2}$, where $L_i = [l_1, l_2, l_3, l_4]^T$ is such that $s^4 + l_1 s^3 + l_2 s^2 + l_3 s + l_4$ is a Hurwitz polynomial. There exists $\bar{\eta}$, $0 < \bar{\eta} \le 1$, such that $\forall \eta \in (0, \bar{\eta})$, $\hat{x} \to x$ as $t \to \infty$.

Proof: See [9].

C. Controller Design

Assumption 6: There exist known constants $g_{ijkU} > 0$ such that $\|g_{ijk}(\cdot)\| \le g_{ijkU}$, $\forall i = 1, 2, 3,\ \forall j = 1, 2,\ \forall k = 1, 2$.

Assumption 7: $x_{1d} \in C^2 \cap L_{\infty e}^2$ is a vector of desired trajectory.

Assumption 8: There exist unknown constants $x_{ijU} > 0$ such that $\|\dot{\hat{x}}_{ij}\| \le x_{ijU}$, $\forall i = 1, \ldots, 4,\ \forall j = 1, 2$.

Assumption 9: There exist unknown constants $T_{iU} > 0$ such that $\|T_i - u_i\| \le T_{iU}$, $\forall i = 1, 2$.

The control objective is to make output, x_1, follow desired trajectory x_{1d} as closely as possible, while all the signals in the closed-loop systems are bounded. We propose the following controller for the system in (2.5). For convenience, arguments are dropped where appropriate.

Proposition 2: Consider the closed-loop system consisting of the plant (2.5), the observer (3.4), the identifier (3.1), the deadzone model (2.3), the backlash model (2.4), and the controller as follows:

$$\begin{aligned} x_{2d} &= -c_1 z_1 + \dot{x}_{1d} = [x_{2d1}, x_{2d2}]^T, \\ x_{3d} &= -\hat{g}_2^{-1}[g_{1U} z_1 + c_2 z_2 + \hat{f}_2 - \dot{x}_{2d} - u_{3dvsc}] = [x_{3d1}, x_{3d2}]^T, \\ x_{4d} &= -g_{2U} z_2 - c_3 z_3 + \dot{x}_{3d} = [x_{4d1}, x_{4d2}]^T, \\ u &= -\hat{g}_4^{-1}[g_{3U} z_3 + c_4 z_4 + \hat{f}_4 - \dot{x}_{4d} - u_{5dvsc}] = [u_1, u_2]^T, \end{aligned} \tag{3.5}$$

where

$$z_i = \hat{x}_i - x_{id}, \ \forall i = 1, \ldots, 4,$$

$$g_{iU} = \begin{bmatrix} g_{i11U} & g_{i12U} \\ g_{i21U} & g_{i22U} \end{bmatrix}, \ \forall i = 1, \ldots, 3.$$

The smooth variable structure control terms are as follows: $u_{(i+1)dvsc} = \left[u_{(i+1)dvsc1}, u_{(i+1)dvsc2}\right]^T$, $i = 2, 4$, where

$$u_{(i+1)dvscj} = -\hat{K}_{ij}{}^T \bar{\phi}_{ij},$$

$$\bar{\phi}_{ij} = \begin{bmatrix} \left\| \bar{Z}_{fij} \hat{W}_{fij}^T \hat{S}_{fij}^{'} \right\|_F \frac{2}{\pi} \arctan\left(\frac{z_{ij}}{\eta_{ij}} \left\| \bar{Z}_{fij} \hat{W}_{fij}^T \hat{S}_{fij}^{'} \right\|_F\right); \\ \left\| \hat{S}_{fij}^{'} \hat{V}_{fij}^T \bar{Z}_{fij} \right\| \frac{2}{\pi} \arctan\left(\frac{z_{ij}}{\eta_{ij}} \left\| \hat{S}_{fij}^{'} \hat{V}_{fij}^T \bar{Z}_{fij} \right\|\right); \\ \frac{2}{\pi} \arctan\left(\frac{z_{ij}}{\eta_{ij}}\right); \\ \sum_{k=1}^{2} \left\{ \left\| \bar{Z}_{g_{ijk}} \hat{W}_{g_{ijk}}^T \hat{S}_{g_{ijk}}^{'} x_{(i+1)dk} \right\|_F \right\} \bullet \\ \frac{2}{\pi} \arctan\left(\frac{z_{ij}}{\eta_{ij}} \sum_{k=1}^{2} \left\{ \left\| \bar{Z}_{g_{ijk}} \hat{W}_{g_{ijk}}^T \hat{S}_{g_{ijk}}^{'} x_{(i+1)dk} \right\|_F \right\}\right); \\ \sum_{k=1}^{2} \left\{ \left\| \hat{S}_{g_{ijk}}^{'} \hat{V}_{g_{ijk}}^T \bar{Z}_{g_{ijk}} x_{(i+1)dk} \right\| \right\} \bullet \\ \frac{2}{\pi} \arctan\left(\frac{z_{ij}}{\eta_{ij}} \sum_{k=1}^{2} \left\{ \left\| \hat{S}_{g_{ijk}}^{'} \hat{V}_{g_{ijk}}^T \bar{Z}_{g_{ijk}} x_{(i+1)dk} \right\| \right\}\right); \\ \sum_{k=1}^{2} \left\{ \left\| x_{(i+1)dk} \right\| \right\} \frac{2}{\pi} \arctan\left(\frac{z_{ij}}{\eta_{ij}} \sum_{k=1}^{2} \left\{ \left\| x_{(i+1)dk} \right\| \right\}\right) \end{bmatrix},$$

η_{ij} is a small positive number. $\hat{K}_{ij}$ approximates K_{ij}^* where

$$\begin{aligned} K_{ij}^* = [&\left\| V_{f_{ij}}^* \right\|_F, \left\| W_{f_{ij}}^* \right\|, \left\| W_{f_{ij}}^* \right\|_1 + \varepsilon_{f_{ijU}} + x_{ijU} + \sum_{k=1}^{2} \left\{ g_{ijkU} d_{aikU} \right\}, \\ &\sum_{k=1}^{2} \left\{ \left\| V_{g_{ijk}}^* \right\|_F \right\}, \sum_{k=1}^{2} \left\{ \left\| W_{g_{ijk}}^* \right\| \right\}, \sum_{k=1}^{2} \left\{ \left\| W_{g_{ijk}}^* \right\|_1 \right\} + \sum_{k=1}^{2} \left\{ \varepsilon_{g_{ijkU}} \right\}]^T. \end{aligned} \tag{3.6}$$

We use the following σ-modification weight updating laws:

$$\dot{\hat{W}}_{fij} = \Gamma_{wfij} [(\hat{S}_{fij} - \hat{S}_{fij}^{'} \hat{V}_{fij}^T \bar{Z}_{fij}) z_{ij} - \sigma_{wfij} \hat{W}_{fij}],$$

$$\dot{\hat{V}}_{fij} = \Gamma_{vfij} [\bar{Z}_{fij} \hat{W}_{fij}^T \hat{S}_{fij}^{'} z_{ij} - \sigma_{vfij} \hat{V}_{fij}],$$

$$\dot{\hat{W}}_{gijk} = \Gamma_{wgijk} [(\hat{S}_{gijk} - \hat{S}_{gijk}^{'} \hat{V}_{gijk}^T \bar{Z}_{gijk}) x_{(i+1)dk} z_{ij} - \sigma_{wgijk} \hat{W}_{gijk}],$$

$$\dot{\hat{V}}_{gijk} = \Gamma_{vgijk} [\bar{Z}_{gijk} \hat{W}_{gijk}^T \hat{S}_{gijk}^{'} x_{(i+1)dk} z_{ij} - \sigma_{vgijk} \hat{V}_{gijk}],$$

$$\dot{\hat{K}}_{ij} = \Gamma_{kij} [\bar{\phi}_{ij} z_{ij} - \sigma_{kij} \hat{K}_{ij}], \text{ where}$$

$$\Gamma_{wfij}, \Gamma_{vfij}, \Gamma_{wgijk}, \Gamma_{vgijk}, \Gamma_{kij} > 0.$$

Assume all the above assumptions hold and assume there exist sufficiently large compact sets such that all input signals of all neural networks belong to these sets at all times. Then, for bounded initial conditions, we have that all system states ($x_i, \forall i = 1, \ldots, 4$), output ($y$), estimated weights ($\hat{W}_{gijk}, \hat{V}_{gijk}, \hat{W}_{fij}, \hat{V}_{fij}, \hat{K}_{ij}$), virtual control inputs ($x_{id}, i = 2, \ldots, 4$), and actual control input (T) are uniformly ultimately bounded. Moreover, all errors ($z_i, \tilde{W}_{gijk}, \tilde{V}_{gijk}, \tilde{W}_{fij}, \tilde{V}_{fij}, \tilde{K}_{ij}$) eventually converge to the compact set

$$\Omega \triangleq \left\{ z_i, \tilde{W}_{gijk}, \tilde{V}_{gijk}, \tilde{W}_{fij}, \tilde{V}_{fij}, \tilde{K}_{ij} \middle| V_m \le \frac{\delta}{\varsigma} \right\},$$

where $\varsigma = \min_{1 \le i \le m} \{2\lambda_{\min}(c_i)\} > 0$, $\delta = \sum_{i=1}^{m} \xi_i \ge 0$,

$$\begin{aligned} \xi_i = \sum_{j=1}^{2} \Big\{ & 0.2785 \eta_{ij} [\left\| V_{f_{ij}}^* \right\|_F + \left\| W_{f_{ij}}^* \right\| + \left\| W_{f_{ij}}^* \right\|_1 + \varepsilon_{f_{ijU}} \\ & + \sum_{k=1}^{2} \left\{ g_{ijkU} d_{aikU} \right\} + \sum_{k=1}^{2} \left\{ \left\| V_{g_{ijk}}^* \right\|_F \right\} + \sum_{k=1}^{2} \left\{ \left\| W_{g_{ijk}}^* \right\| \right\} + \sum_{k=1}^{2} \left\{ \left\| W_{g_{ijk}}^* \right\|_1 \right\} \\ & + \sum_{k=1}^{2} \left\{ \varepsilon_{g_{ijkU}} \right\}] \Big\} + \sum_{j=1}^{2} \sum_{k=1}^{2} \left\{ + \frac{\sigma_{wgijk}}{2} \left\| W_{gijk}^* \right\|^2 \right\} \\ & + \sum_{j=1}^{2} \sum_{k=1}^{2} \left\{ + \frac{\sigma_{vgijk}}{2} \left\| V_{gijk}^* \right\|_F^2 \right\} + \sum_{j=1}^{2} \left\{ + \frac{\sigma_{wfij}}{2} \left\| W_{fij}^* \right\|^2 \right\} \\ & + \sum_{j=1}^{2} \left\{ + \frac{\sigma_{vfij}}{2} \left\| V_{fij}^* \right\|_F^2 \right\} + \sum_{j=1}^{2} \left\{ + \frac{\sigma_{kij}}{2} \left\| K_{ij}^* \right\|^2 \right\}. \end{aligned}$$

Proof: See [9].

IV. Simulation Results

To represent an actual physical system as closely as possible, parameters of the plant dynamic model (2.1) used in our simulation are obtained from real experiments with the following results:

$$M(q_1) = \begin{bmatrix} 0.201 + 0.06\cos\theta_2 & 0.0266 + 0.03\cos\theta_2 \\ 0.0266 + 0.03\cos\theta_2 & 0.0266 \end{bmatrix},$$

$$J = \begin{bmatrix} 0.017 & 0 \\ 0 & 0.014 \end{bmatrix},$$

$$V(q_1, \dot{q}_1) = \begin{bmatrix} 0 & -0.03(2\dot{\theta}_1 + \dot{\theta}_2)\sin\theta_2 \\ 0.03\dot{\theta}_1 \sin\theta_2 & 0 \end{bmatrix},$$

$$K = \begin{bmatrix} 0.4 & 0 \\ 0 & 0.4 \end{bmatrix}, \ B = \begin{bmatrix} 0.003 & 0 \\ 0 & 0.003 \end{bmatrix}.$$

Parameters used in friction model (2.2) are as follows: $\sigma_0 = 0.01, \sigma_1 = 0.1, F_c = 10, F_s = 20, v_s = 0.1, \quad \sigma_2 = 0.02$ for $F(\dot{\theta}_1), F(\dot{\theta}_2)$ and $\sigma_2 = 0.056$ for $F(\dot{\theta}_5), F(\dot{\theta}_6)$.

Parameters used in deadzone model (2.3) are as follows: $d_- = -0.1, d_+ = 0.1, h_1(u) = (u - d_-), h_2(u) = (u - d_+)$.

Parameters used in backlash model (2.4) are as follows: $d^- = -0.1, d^+ = 0.1, m = 1$.

External disturbances that appear in (2.5) are as follows:

$$d_{a1} = d_{a4} = [0.01\sin(\theta_1\dot{\theta}_1), \arctan(\theta_1\dot{\theta}_2)]^T,$$
$$d_{a2} = d_{a3} = [0.01\text{randn}(2,1)]^T,$$

where *randn* represents white noise.

To simulate payload changes, all elements in the matrices M, V above are multiplied by a factor of 3 during simulation periods from 1 to 6 s and 11 to 16 s.

It can be verified that this system satisfies all required assumptions of the proposed control scheme. Only the output, $y = [\theta_1, \theta_2]^T$, is measured and all nonlinear functions are assumed unknown. The control objective is to guarantee that (i) all closed-loop signals remain bounded, and (ii) the output *y* follow the desired trajectory generated by passing a square wave of amplitude 10 and 5, for θ_1 and θ_2 respectively, with zero mean, and 20-s period into the filter $1/(s+2)^3$. Number of hidden-layer nodes is 3. The observer and controller are as in Section III. All design parameters are as follows:

$$\Gamma_{wfi} = \Gamma_{vfi} = \Gamma_{wgi} = \Gamma_{vgi} = 10, \ \Gamma_{ki} = 1,$$
$$c_i = 15, \ \sigma_{wfi} = \sigma_{vfi} = \sigma_{wgi} = \sigma_{vgi} = \sigma_{ki} = 0.1, \ \forall i = 2,4,$$
$$\eta = 0.1, \ L_j = [16, 91, 216, 180]^T, \ \forall j = 1,2.$$

Sampling period is 1 ms. Saturation limit of control inputs is set at ± 50 Nm. All initial values are set to 0.1. Simulation results are as shown in Fig. 6 to 8. We can see from Fig. 6 and 7 that the controller achieves good tracking performance of both θ_1 and θ_2 even if payload is changed during the two time intervals from 1 to 6 s and 11 to 16 s. This results from good observer and controller performance as seen in Figures 7 and 8, parts (c) and (e), respectively. Actual control inputs are bounded as shown in Fig. 8.

To have a brief idea of how much each component in the control system contributes to the overall tracking performance, several plots are provided in Fig. 5. We compare four situations: a) when the observer is not used, b) when the identifier is not used, c) when both observer and identifier are not used, and d) when both observer and identifier are used. We can see that the tracking performance of this controller is comparable to that obtained in the ideal case.

V. Conclusion

Analysis as well as simulation using a rather complete model of a two-link flexible-joint manipulator shows the effectiveness of the proposed backstepping neural network observer-controller design scheme. It should be noted that this design scheme can handle uncertainties very well both from additive disturbances and from unknown nonlinear functions, which can be time-varying or contain unmodeled dynamics.

References

[1] M. C. Good, L. M. Sweet and K. L. Strobel, "Dynamic models for control system design of integrated robot and drive systems," *Journal of Dynamic Systems Measurement & Control*, vol. 107, no. 1, pp.53-9, March 1985.

[2] F.L. Lewis, J. Campos and R. Selmic, *Neuro-Fuzzy Control of Industrial Systems with Actuator Nonlinearities*. Philadelphia: SIAM, 2002.

[3] B. Brogliato, R. Ortega and R. Lozano, "Global tracking controllers for flexible-joint manipulators: a comparative study," *Automatica*, vol. 31, no. 7, pp. 941-956, July 1995.

[4] S.S. Ge, T.H. Lee and C.J. Harris, *Adaptive Neural Network Control of Robotic Manipulators*. Singapore: World Scientific Publishing, 1998.

[5] J. Hernandez and J. P. Barbot, "Sliding observer-based feedback control for flexible joints manipulator," *Automatica*, vol. 32, no. 9, pp. 1243-1254, September 1996.

[6] H. D. Taghirad and G. Bakhshi, "Composite-H_∞ controller synthesis for flexible joint robots," in *Proc. 2002 IEEE/RSJ Intl. Conf. on Intelligent Robots and Systems*, Switzerland, 2002, pp. 2067-2072.

[7] C. W. Park and Y. W. Cho, "Adaptive tracking control of flexible joint manipulator based on fuzzy model reference approach," in *IEE Proc. Control Theory and Applications*, 2003, pp. 198-204.

[8] F. Abdollahi, H. A. Talebi and R. V. Patel, "A stable neural network observer with application to flexible-joint manipulators," in *Proc. 9th International Conf. on Neural Information Processing*, 2002, pp. 1910-1914.

[9] W. Chatlatanagulchai, and P. H. Meckl, "Robust observer backstepping neural network control of nonlinear systems in strict feedback form," in *Proc. American Control Conference*, Boston, 2004, to be published.

[10] H. Nho, "An experimental and theoretical study of various control approaches to flexible-joint robot manipulator undergoing payload changes," Motion and Vibration Control Lab. Report, School of Mechanical Engineering, Purdue University, 2003.

[11] M. W. Spong, "Modeling and control of elastic joint robots," *Journal of Dynamic Systems Measurement & Control-Transactions of the ASME*, vol. 109, no. 4, pp. 310-319, December 1987.

[12] G. Tao and P. V. Kokotovic, *Adaptive Control of Systems with Actuator and Sensor Nonlinearities*. New York: Wiley, 1996.

[13] C. Canudas, H. Olsson, K. J. Astrom and P. Lischinsky, "A new model for control of systems with friction," *IEEE Trans. Automat. Contr.*, vol. 40, no. 3, pp. 419-425, March 1995.

[14] K. Hornik, M. Stinchcombe and H. White, "Multilayer feedforward networks are universal approximators," *Neural Networks*, vol. 2, pp. 359-366.

[15] S. S. Ge, C. C. Hang, T. H. Lee and T. Zhang, *Stable Adaptive Neural Network Control*. The Netherlands: Kluwer, 2002, ch. 2.

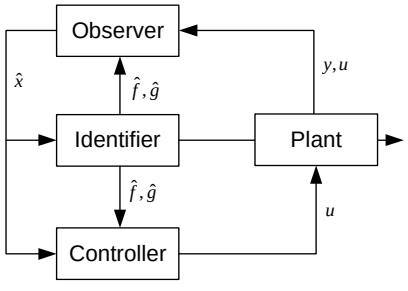

Fig. 1. Observer-identifier-controller system diagram.

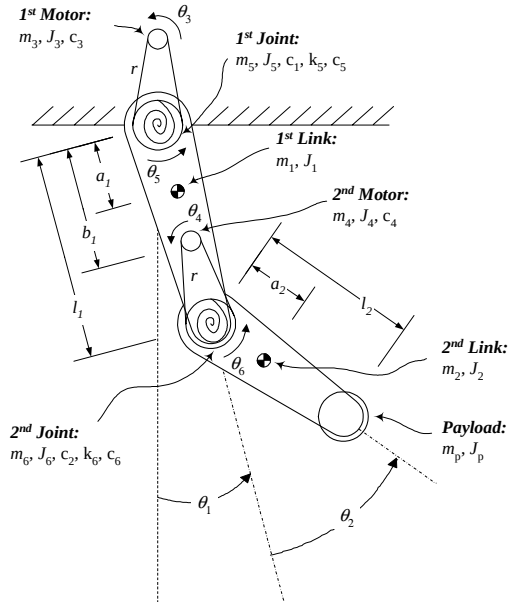

Fig. 2. Schematic diagram of planar two-link flexible-joint manipulator.

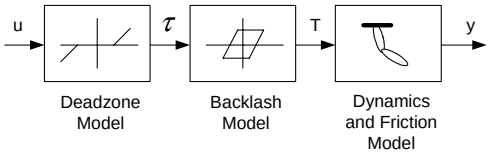

Fig. 3. Overall plant model.

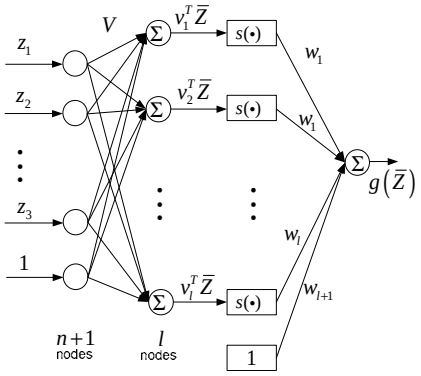

Fig. 4. A 3-layer neural network.

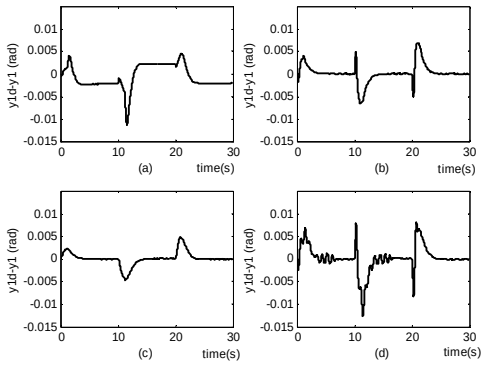

Fig. 5. Overall tracking error ($\theta_1 - \theta_{1d}$) comparison: (a) when observer is not used (measured states, unknown plant). (b) when identifier is not used (unmeasured states, known plant). (c) when both observer and identifier are not used (measured states, known plant). (d) when both observer and identifier are used (unmeasured states, unknown plant).

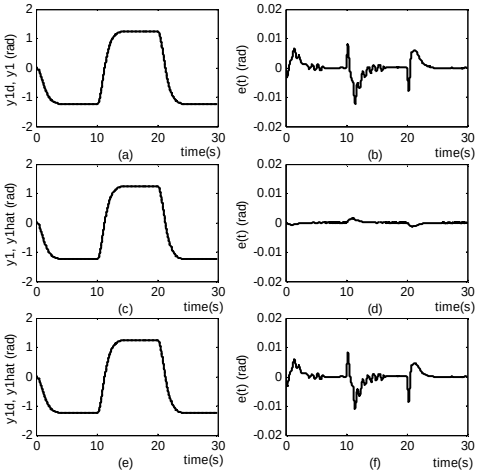

Fig. 6. Tracking performance during 30 s: (a) θ_1 versus θ_{1d}, (b) error $\theta_1 - \theta_{1d}$, (c) θ_1 versus $\hat{\theta}_1$, (d) error $\theta_1 - \hat{\theta}_1$, (e) $\hat{\theta}_1$ versus θ_{1d}, (f) error $\hat{\theta}_1 - \theta_{1d}$.

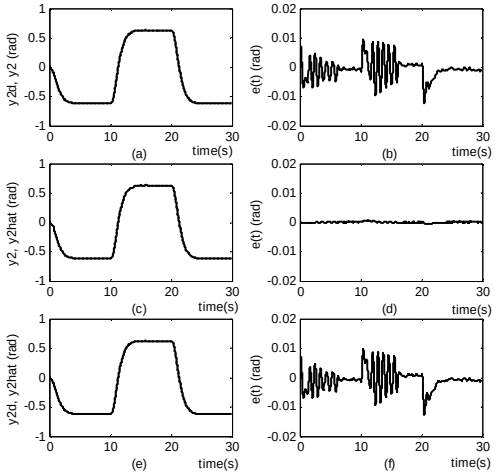

Fig. 7. Similar to previous figure but with $\theta_2, \theta_{2d}, \hat{\theta}_2$.

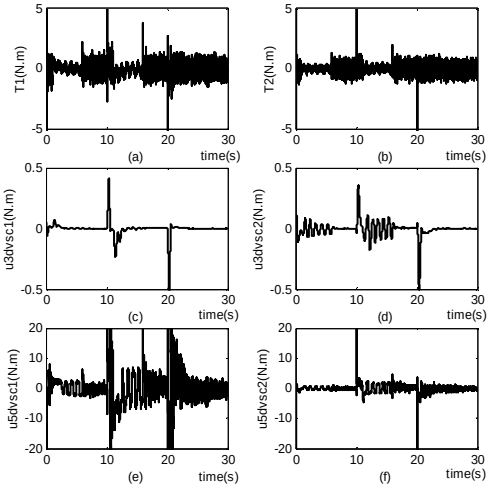

Fig. 8. Control input during 30 s: (a) torque T_1, (b) torque T_2, (c) variable structure control input u_{3dvsc1}, (d) u_{3dvsc2}, (e) u_{5dvsc1}, (f) u_{5dvsc2}.